Inorganic Chemistry

Communication

pubs.acs.org/IC

Evaluation of a Ruthenium Oxyquinolate Architecture for Dye-Sensitized Solar Cells

Helen C. Zhao,[†] Joseph P. Harney,[†] Yu-Ting Huang,[‡] Jun-Ho Yum,[§] Md. K. Nazeeruddin,[§] Michael Grätzel,[§] Ming-Kang Tsai,[‡] and Jonathan Rochford*[,†]

[†]Department of Chemistry, University of Massachusetts—Boston, 100 Morrissey Boulevard, Boston, Massachusetts 02125, United States

[‡]Department of Chemistry, National Taiwan Normal University, Taipei, Taiwan, Republic of China

[§]Laboratory for Photonics and Interfaces, Institute of Chemical Sciences and Engineering, School of Basic Sciences, Swiss Federal Institute of Technology, CH-1015 Lausanne, Switzerland

S *Supporting Information*

ABSTRACT: Synthesis of the $[Ru(dcbpy)_2(OQN)]^+$ complex is reported in which dcbpy and OQN^- are the bidentate 4,4′-dicarboxy-2,2′-bipyridyl and 8-oxyquinolate ligands, respectively. Spectroscopic, electrochemical, and theoretical analyses are indicative of extensive Ru(OQN) molecular orbital overlap due to degenerate Ru d(π) and OQN p(π) mixing. $[Ru(dcbpy)_2(OQN)]^+$ displays spectroscopic properties remarkably similar to those of the N3 dye, making it a promising candidate for application in dye-sensitized solar cell devices. However, its solar power conversion efficiency requires further optimization.

The development of clean, renewable, alternative energy technologies is anticipated to solve the problems associated with rising atmospheric CO_2 levels and the depletion of fossil fuel resources. One promising candidate for solar-to-electricity conversion is the dye-sensitized solar cell (DSSC) developed by Grätzel and co-workers over 20 years ago.[1] First reported by Nazeeruddin et al. in 1993, the $Ru(dcbpy)_2(NCS)_2$ complex, commonly known as the N3 dye (Figure 1), has become a benchmark ruthenium-based chromophore in the DSSC field because of its ease of preparation and its high efficiency (η = 10.4%).[2] Many reports inspired by the N3 dye have involved the replacement of one dcbpy ligand to produce complexes of the general structure $Ru(dcbpy)(L)(NCS)_2$, where L is typically a bidentate 2,2′-bipyridyl ligand with highly conjugated electron-donating substituents in the 4 and 4′ positions. In fact, one of the largest efficiencies reported for a DSSC device is held by such a ruthenium-based dye, C106, with η = 12.10%.[3] In contrast, there have been few attempts to replace the monodentate NCS^- ligands of the N3 dye.[4] Recently, Bessho et al. replaced both NCS^- ligands of the N3 dye with a chelating orthometalated ligand, 2-(2,4-difluorophenyl)pyridine, producing the YE05 dye, which has a solar-to-power conversion efficiency of η = 10.1%. Berlinguette and co-workers have since expanded upon this series of orthometalated dyes, with initial efforts achieving efficiencies in the range of 2−4%. Inspired by this approach, we have begun a study of bisheteroleptic ruthenium complexes containing the bidendate 8-oxyquinolate (OQN^-) ligand. Of further interest in this study is the noninnocent nature of the OQN^- ligand.[5]

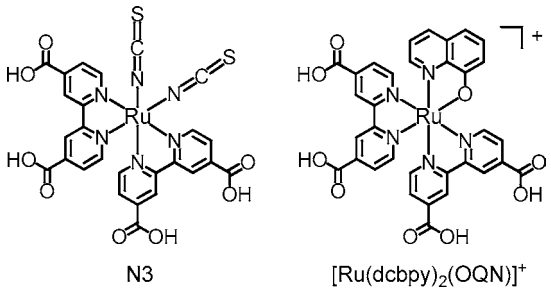

Figure 1. Structures of complexes investigated in this study.

Ruthenium(II) polypyridyl complexes typically display an intense electronic transition in the visible region of the spectrum due to two closely spaced $Ru^{II}(t_{2g}) \rightarrow bpy(\pi^*)$ singlet metal-to-ligand charge-transfer (^{1}MLCT) excitations with the standard complex $[Ru^{II}(bpy)_3]^{2+}$ characterized by an extinction coefficient of ε = 14 650 M^{-1} cm^{-1} at 453 nm in methanol. Incorporation of the OQN^- ligand into the ruthenium coordination sphere causes dramatic changes to its electronic structure, which has important consequences for its light-harvesting properties toward application in solar energy conversion.

The UV−vis absorption spectrum of $[Ru(dcbpy)_2(OQN)]^+$ on TiO_2 displays an extraordinary resemblance to that of the N3 dye even though both monodentate NCS^- ligands are replaced by the bidentate OQN^- ligand (Figure S3 in the Supporting Information, SI). Two intense electronic transitions (Figure 2) are observed in the visible region at 393 nm (ε = 14 600 M^{-1} cm^{-1}) and 535 nm (ε = 12 900 M^{-1} cm^{-1}). An additional absorption is observed at 469 nm (ε = 9600 M^{-1} cm^{-1}). A similar absorption is observed upon adsorption of N3 to TiO_2 (Figure S3 in the SI)[1] and also for the YE05 dye, which is comparable both structurally and electronically to $[Ru(dcbpy)_2(OQN)]^+$.[4d] In fact, each of the OQN^-, 2-(2,4-difluorophenyl)pyridine, and NCS^- ligands imparts similar

Received: June 27, 2011
Published: November 30, 2011

   dx.doi.org/10.1021/ic201375k | *Inorg. Chem.* 2012, 51, 1−3

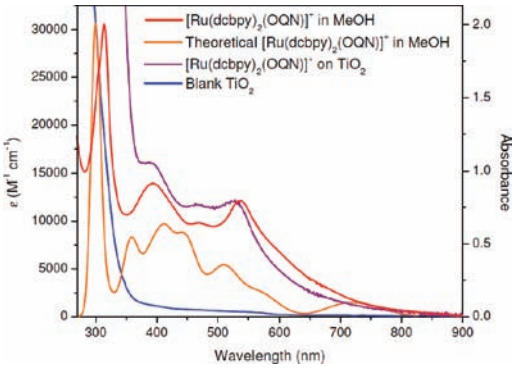

Figure 2. UV−vis absorption spectra for $[Ru(dcbpy)_2(OQN)]^+$ recorded in methanol (ε, left y axis), chemisorbed on TiO_2 (abs, right y axis), and overlaid with blank TiO_2 (abs, right y axis). The theoretical time-dependent density functional theory spectrum of $[Ru(dcbpy)_2(OQN)]^+$ in methanol is normalized with the experimental spectrum in methanol at 300 nm.

properties on the $Ru(dcbpy)_2$ core by introducing a substantial ligand contribution to the highest occupied molecular orbital (HOMO) by degenerate mixing of Ru d(π) and ligand p(π) orbitals (Table 1 and Figure 3).[4d] Such metal−ligand

Table 1. Character Table of Selected Electronic Transitions for $[Ru(dcbpy)_2(OQN)]^+$ Calculated by the Time-Dependent Density Functional Theory

electronic transition (nm)	occupied orbitals	empty orbitals	contributions (%)
414.36	H−1	L+2	77
439.66	H	L+6	33
	H−3	L+1	26
512.98	H	L+3	68
	H−2	L	15
716.25	H	L+1	76
	H	L	19

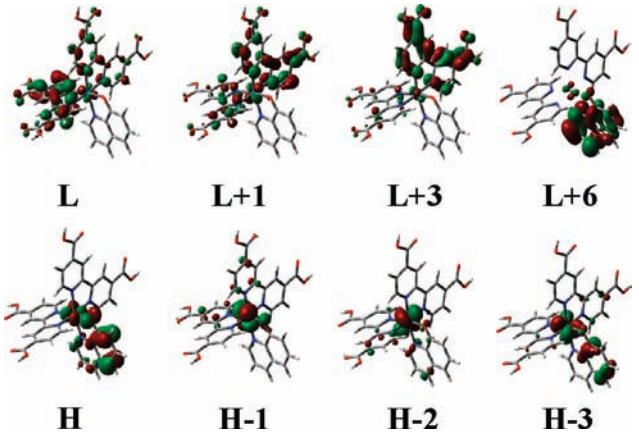

Figure 3. Selection of molecular orbitals for the $[Ru(dcbpy)_2(OQN)]^+$ sensitizer with H−3, H, and L+6 exhibiting extensive Ru d(π) and OQN p(π) mixing (H = HOMO; L = LUMO).

interaction is anticipated to allow for stabilization of the oxidized dye, following photoinjection into the TiO_2 conduction band, via extensive delocalization of the photogenerated electron−hole between the ruthenium and ligand π orbitals. Evidence for this noninnocent ligand character is borne out by electrochemical and theoretical analyses.

A theoretical investigation of $[Ru(dcbpy)_2(OQN)]^+$ confirms the presence of multiple underlying transitions in its visible absorption spectrum consistent with C_1 symmetry (Table 1). For example, the intense low-energy transition observed at λ_{max} = 535 nm consists primarily of a HOMO → LUMO+3 transition with a significant contribution from a HOMO−2 → LUMO transition. The HOMO orbital is largely delocalized across the Ru(OQN) π framework (Figure 3), with the LUMO and LUMO+3 molecular orbitals largely consisting of dcbpy π^* character. The 535 nm absorption band tails off to ca. 900 nm because of a broad, weak underlying transition consisting of significant HOMO → LUMO+1 and partial HOMO → LUMO character. The higher energy intense transition observed at 393 nm consists primarily of HOMO−2 → LUMO+2 character. The intermittent transition at 469 nm has substantial character from the HOMO → LUMO+6 transition, where the LUMO+6 orbital is located on the pyridyl side of the OQN^- ligand.

Cyclic voltammetry of $[Ru(dcbpy)_2(OQN)]^+$ was conducted to further investigate its electronic properties and its potential as a DSSC sensitizer. $[Ru(bpy)_3]^{2+}$, $[Ru(bpy)_2(OQN)]^+$, and the N3 dye were also investigated for reference purposes (Table 2 and Figures S4 and S5 in the SI). For example,

Table 2. Electrochemical Data for $[Ru(dcbpy)_2(OQN)]^+$ and Reference Compounds (1 mM) Recorded in DMF Electrolyte (0.1 M Bu_4NPF_6)

	$E_{1/2}$ (vs NHE)			
	oxidation	reduction		
$[Ru(bpy)_3]^{2+}$	+1.51	−1.03	−1.21	−1.47
$[Ru(bpy)_2(OQN)]^+$	+0.78	−1.20	−1.45	−2.01
N3	+1.13[a]	−0.89[a]	−1.14[a]	~
$[Ru(dcbpy)_2(OQN)]^+$	+0.80	−1.20	−1.47	−1.92[a]
YE05[4d]	+1.08	−1.20		

[a]Estimated from the square-wave voltammogram due to irreversibility.

$[Ru(bpy)_2(OQN)]^+$ shows a strong cathodic shift of 0.73 V for its first oxidation relative to $[Ru(bpy)_3]^{2+}$. This is explained by the strong mixing of Ru d(π) orbitals with the electron-rich OQN p(π) orbitals. Oxidation of $[Ru(dcbpy)_2(OQN)]^+$ is best described as a $[Ru(OQN)]^{2+/+}$ couple (Scheme 1); i.e., this

Scheme 1. Resonance Forms of $[Ru(dcbpy)_2(OQN)]^{2+}$ Demonstrating the Noninnocent Behavior of the OQN^- Ligand

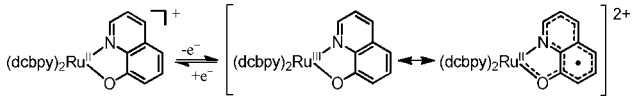

cannot be described as a localized $Ru^{III/II}$ couple as in the case of $[Ru(bpy)_3]^{2+}$. Of particular note is the reversibility of this redox couple relative to that of the N3 dye (Figure S5 in the SI).

In the negative potential region, as anticipated, two sequential one-electron dcbpy-based reductions are observed for $[Ru(dcbpy)_2(OQN)]^+$. Reduction of the electron-rich OQN^- ligand is significantly more negative of dcbpy and is typically irreversible at $E_{1/2}$ = −1.92 V. The latter is suggested as an approximate value because of its irreversible character (Figure S5 in the SI). Analogous to the N3 dye, oxidation of

dx.doi.org/10.1021/ic201375k | Inorg. Chem. 2012, 51, 1−3

$[Ru(dcbpy)_2(OQN)]^+$ shows an anodic shift of +0.06 V upon adsorption to TiO_2 (Figure 4).

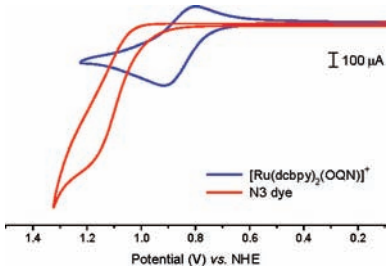

Figure 4. Cyclic voltammograms of $[Ru(dcbpy)_2(OQN)]^+$ and N3 chemisorbed on 1 cm^2 TiO_2 electrodes (0.1 M Bu_4NPF_6/DMF; 50 mV s^{-1}).

A poor overall solar-to-electric power conversion of η = 1.84% was observed for $[Ru(dcbpy)_2(OQN)]^+$, primarily because of a low open-circuit potential (Figure 5; V_{OC} = 334 mV;

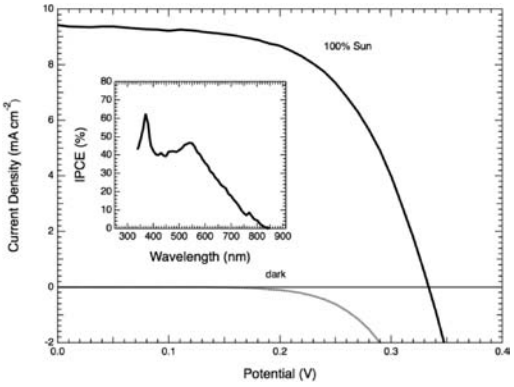

Figure 5. *J*–*V* and IPCE (inset) characteristics of a $[Ru(dcbpy)_2(OQN)]^+$ DSSC (9 + 5 μm TiO_2 film; electrolyte composed of 0.6 M 1,3-dimethylimidazolium iodide, 0.05 M LiI, 0.03 M I_2, in a 15/85 (v/v) mixture of valeronitrile and acetonitrile; active area = 0.185 cm^2).

J_{SC} = 9.42 mA cm^{-2}; ff = 0.59; AM 1.5). This may be attributed to a number of contributing factors. Although absorption spectra indicate a comparable surface coverage of $[Ru(dcbpy)_2(OQN)]^+$ relative to N3 on TiO_2 (Figure S3 in the SI; $\Gamma \sim 6 \times 10^{-8}$ mol cm^{-2}), a reduced current response of the sensitized electrode (Figures 4 and S6 in the SI) suggests poor lateral electron percolation across the TiO_2–$[Ru(dcbpy)_2(OQN)]^+$ interface, indicating a nonuniform packing at the surface.[6] This can be explained by a Coulombic repulsion of the positively charged $[Ru(dcbpy)_2(OQN)]^+$ dye molecules, allowing greater access of Li^+ and I_3^- electrolyte ions to the TiO_2 surface states. Li^+ is well-known to lower the TiO_2 Fermi level.[7] Electrochemical impedance spectra support this hypothesis because increased charge recombination of $TiO_2^{\bullet-}$ conduction band electrons with I_3^- ions (relative to the N3 device) is observed in the Nyquist plot (Figures S10 and S11 in the SI). Furthermore, Bode plots indicate a 15-fold shorter lifetime of electrons in TiO_2 for the $[Ru(dcbpy)_2(OQN)]^+$-based device relative to N3 (Figures S10 and S11 in the SI). It is also possible that charge recombination losses with the oxidized sensitizer at the $TiO_2^{\bullet-}$/$dye^{\bullet+}$ interface may contribute to the poor V_{OC}.[8] This is probably moderate because the $E_{1/2}$ of $[Ru(dcbpy)_2(OQN)]^+$ on TiO_2 (0.86 V; Figure 4), although 0.4 V negative of the N3 dye, still lies 0.55 V positive of the I^-/I_3^- redox mediator ($E_{1/2}$ = +0.31 V).[9] The Fermi level of TiO_2 is also influenced by the dye dipole moment.[10] Although the dipole of N3 (13.69 DB) is almost twice that of $[Ru(dcbpy)_2(OQN)]^+$ (6.89 DB), the latter is greater than that calculated for the efficient YE05 (4.65 DB) dye. Studies are underway to optimize this class of sensitizer for an improved V_{OC} response.

■ ASSOCIATED CONTENT

Ⓢ Supporting Information

Synthesis, characterization, physical methods, computational details, and additional UV–vis, electrochemical, and theoretical data. This material is available free of charge via the Internet at http://pubs.acs.org.

■ AUTHOR INFORMATION

Corresponding Author

*E-mail: jonathan.rochford@umb.edu.

■ ACKNOWLEDGMENTS

J.R. thanks University of Massachusetts—Boston for financial support. Y.-T.H. and M.-K.T. are supported by the National Science Council of Taiwan (Grant 99-2113-M-003-007-MY2) and thank the National Center for High-performance Computing in Taiwan for computer time.

■ REFERENCES

(1) Vlachopoulos, N.; Liska, P.; Augustynski, J.; Gratzel, M. *J. Am. Chem. Soc.* **1988**, *110*, 1216–1220.

(2) Nazeeruddin, M. K.; Kay, A.; Rodicio, I.; Humphrybaker, R.; Muller, E.; Liska, P.; Vlachopoulos, N.; Gratzel, M. *J. Am. Chem. Soc.* **1993**, *115*, 6382–6390.

(3) Yu, Q.; Wang, Y.; Yi, Z.; Zu, N.; Zhang, J.; Zhang, M.; Wang, P. *ACS Nano* **2010**, *4*, 6032–6038.

(4) (a) Argazzi, R.; Bignozzi, C. A.; Hasselmann, G. M.; Meyer, G. J. *Inorg. Chem.* **1998**, *37*, 4533–4537. (b) Islam, A.; Sugihara, H.; Arakawa, H. *J. Photochem. Photobiol. A: Chem.* **2003**, *158*, 131–138. (c) Islam, A.; Sugihara, H.; Hara, K.; Singh, L. P.; Katoh, R.; Yanagida, M.; Takahashi, Y.; Murata, S.; Arakawa, H. *J. Photochem. Photobiol. A: Chem.* **2001**, *145*, 135–141. (d) Bessho, T.; Yoneda, E.; Yum, J. H.; Guglielmi, M.; Tavernelli, I.; Imai, H.; Rothlisberger, U.; Nazeeruddin, M. K.; Gratzel, M. *J. Am. Chem. Soc.* **2009**, *131*, 5930–5934. (e) McCall, K. L.; Jennings, J. R.; Wang, H.; Morandeira, A.; Peter, L. M.; Durrant, J. R.; Yellowlees, L. J.; Woollins, J. D.; Robertson, N. *J. Photochem. Photobiol. A: Chem.* **2009**, *202*, 196–204. (f) Bomben, P. G.; Robson, K. C. D.; Sedach, P. A.; Berlinguette, C. P. *Inorg. Chem.* **2009**, *48*, 9631–9643. (g) Bomben, P. G.; Koivisto, B. D.; Berlinguette, C. P. *Inorg. Chem.* **2010**, *49*, 4960–4971. (h) McCall, K. L.; Morandeira, A.; Durrant, J.; Yellowlees, L. J.; Robertson, N. *Dalton Trans.* **2010**, *39*, 4138–4145. (i) Bomben, P. G.; Theriault, K. D.; Berlinguette, C. P. *Eur. J. Inorg. Chem.* **2011**, 1806–1814.

(5) (a) Sears, R. B.; Joyce, L. E.; Turro, C. *Photochem. Photobiol.* **2010**, *86*, 1230–1236. (b) Boyer, J. L.; Rochford, J.; Tsai, M. K.; Muckerman, J. T.; Fujita, E. *Coord. Chem. Rev.* **2010**, *254*, 309–330.

(6) Bonhote, P.; Gogniat, E.; Tingry, S.; Barbe, C.; Vlachopoulos, N.; Lenzmann, F.; Comte, P.; Gratzel, M. *J. Phys. Chem. B* **1998**, *102*, 1498–1507.

(7) (a) Haque, S. A.; Palomares, E.; Cho, B. M.; Green, A. N. M.; Hirata, N.; Klug, D. R.; Durrant, J. R. *J. Am. Chem. Soc.* **2005**, *127*, 3456–3462. (b) Koops, S. E.; O'Regan, B. C.; Barnes, P. R. F.; Durrant, J. R. *J. Am. Chem. Soc.* **2009**, *131*, 4808–4818.

(8) O'Regan, B. C.; Scully, S.; Mayer, A. C.; Palomares, E.; Durrant, J. *J. Phys. Chem. B* **2005**, *109*, 4616–4623.

(9) Oskam, G.; Bergeron, B. V.; Meyer, G. J.; Searson, P. C. *J. Phys. Chem. B* **2001**, *105*, 6867–6873.

(10) Pandey, S. S.; Lee, K.-Y.; Hayat, A.; Ogomi, Y.; Hayase, S. *Jpn. J. Appl. Phys.* **2011**, 50.